

RESEARCH ARTICLE

Recent trend in the global distribution of aerosol direct radiative forcing from satellite measurements

Tamanna Subba^{1,3}  | Mukunda M. Gogoi²  | Binita Pathak^{3,4} | Pradip K. Bhuyan³  | S. Suresh Babu²

¹Climate and Space Sciences and Engineering, University of Michigan, Ann Arbor, Michigan

²Space Physics Laboratory, Vikram Sarabhai Space Centre, Thiruvananthapuram, India

³Centre for Atmospheric Studies, Dibrugarh University, Dibrugarh, India

⁴Department of Physics, Dibrugarh University, Dibrugarh, India

Correspondence

Mukunda M. Gogoi, Space Physics Laboratory, Vikram Sarabhai Space Centre Indian Space Research Organization, Thiruvananthapuram 695022, India.

Email: dr_mukunda@vssc.gov.in

Funding information

Indian Space Research Organisation, Grant/Award Number: ISRO-GBP

Abstract

Global distribution of aerosol direct radiative forcing (DRF) is estimated using Clouds and Earth's Radiant Energy System (CERES) synoptic (SYN) 1° datasets. During 2001–2017, a statistically significant change of global DRFs is revealed with a general decreasing trend (i.e., a reduced cooling effect) at the top of the atmosphere ($DRF_{TOA} \sim 0.017 \text{ W}\cdot\text{m}^{-2}\cdot\text{year}^{-1}$) and at the surface ($DRF_{SFC} \sim 0.033 \text{ W}\cdot\text{m}^{-2}\cdot\text{year}^{-1}$) with rapid change over the land compared to the global ocean. South Asia and Africa/Middle East regions depict significant increasing trend of atmospheric warming by 0.025 and 0.002 $\text{W}\cdot\text{m}^{-2}\cdot\text{year}^{-1}$ whereas, the rest of the regions show a decline. These regional variations significantly modulate the global mean DRF ($-5.36 \pm 0.04 \text{ W}\cdot\text{m}^{-2}$ at the TOA and $-9.64 \pm 0.07 \text{ W}\cdot\text{m}^{-2}$ at the surface during the study period). The observed DRF trends are coincident with the change in the underlying aerosol properties, for example, aerosol optical depth, Ångström exponent and partly due to the increasing columnar burden of SO_2 over some of the regions. This indicates that increasing industrialization and urbanization have caused prominent change in the DRF during recent decades.

KEYWORDS

aerosol optical depth, angstrom exponent, global aerosol radiative forcing, trend

1 | INTRODUCTION

Assessing global distribution of aerosol direct radiative forcing (DRF) and their long-term trends are vital to improve the state of understanding about the significance of aerosol climate forcing as well as the effectiveness of emission control policies (IPCC, 2013; Zhao *et al.*, 2017; Yang *et al.*, 2018; Aas *et al.*, 2019). Study of aerosol radiation interactions are also essential for understanding the changes of the photolysis rates which influences other (viz., O_3 , NO_2 , SO_2) air pollutants (e.g., Li *et al.*, 2014; Xing

et al., 2015). In this regard, extensive measurements and radiative transfer simulations are used to estimate DRFs. However, the global estimation of DRFs has always been challenging especially due to inhomogeneity in both land surface and aerosol properties, posing most uncertain component for the estimation of cumulative radiative forcing (IPCC, 2013; Myhre *et al.*, 2013; Murphy and Ravishankara, 2018). These uncertainties result from the uncertainty in (a) mixing state (including size and density) of aerosols (Seinfeld and Pandis, 2006; Kahn and Gaitley, 2015; Samset *et al.*, 2018), (b) vertical profile of

This is an open access article under the terms of the Creative Commons Attribution License, which permits use, distribution and reproduction in any medium, provided the original work is properly cited.

© 2020 The Authors. *Atmospheric Science Letters* published by John Wiley & Sons Ltd on behalf of the Royal Meteorological Society.

aerosols (Chung *et al.*, 2005), (c) consideration of inaccurate aerosol species contributing to the total forcing in the models (Forster *et al.*, 2007; Murphy, 2013; Myhre *et al.*, 2013; Stevens, 2015; Paulot *et al.*, 2018), their subsequent feedback to climate systems (Stocker *et al.*, 2013); in addition to measurement errors and errors in models itself (IPCC, 2013). Lack of appropriate quantification of anthropogenic fraction of aerosol composites is also accountable to the large fraction of total uncertainty (Su *et al.*, 2018; Myhre *et al.*, 2013). For example, best estimated radiative forcing for the change in the net aerosol radiation interaction between 1,750 and 2005 is associated with a large uncertainty range of -0.85 to $+0.15$ $\text{W}\cdot\text{m}^{-2}$ for the corresponding mean value of -0.35 $\text{W}\cdot\text{m}^{-2}$ (IPCC, 2013).

To reduce the uncertainties in radiative forcing estimation, numerous studies have been made employing the combinations of radiative transfer simulations (e.g., Penner *et al.*, 1994), models (Hansen *et al.*, 1997; Li *et al.*, 2014; Paulot *et al.*, 2018), in-situ measurements (Putaud *et al.*, 2014) and remote sensing observations (Loeb and Kato, 2002; Zhang *et al.*, 2005). In recent years, the global observations of the solar radiation (Christopher and Zhang, 2004; Contreras *et al.*, 2017) and aerosols (Kahn *et al.*, 2005; Remer *et al.*, 2005, 2008; Levy *et al.*, 2009; Moorthy *et al.*, 2013; Babu *et al.*, 2013; Kahn and Gaitley, 2015; Zhao *et al.*, 2017) from space have been used for the accurate estimation of the radiative forcing (Christopher and Zhang, 2004; Bellouin *et al.*, 2005; Patadia *et al.*, 2008; Kahn, 2012). Using the Moderate Resolution Imaging Spectroradiometer (MODIS) and Clouds and the Earth's Radiant Energy System (CERES) data sets, Patadia *et al.* (2008) have found the global clear sky DRF over the land to be -5.1 ± 1.1 $\text{W}\cdot\text{m}^{-2}$. Similarly, Loeb and Kato (2002) used the collocated Visible Infrared Scanner (VIRS) and CERES data to estimate SW DRFs over the tropical oceans (-0.46 $\text{W}\cdot\text{m}^{-2}$). Zhang *et al.* (2005) used CERES and MODIS AODs and estimated SW-DRF over global ocean as -5.3 ± 1.7 $\text{W}\cdot\text{m}^{-2}$ (2000–2001).

The global average aerosol forcing due to both natural and anthropogenic aerosols was found to be -4.3 $\text{W}\cdot\text{m}^{-2}$ at the top of the atmosphere (TOA), $+5.5$ $\text{W}\cdot\text{m}^{-2}$ in the atmosphere (ATM) and -9.7 $\text{W}\cdot\text{m}^{-2}$ at the surface (SFC) (2001–2009, Chung, 2012). Paulot *et al.* (2018) have reported an increase in the DRFs over Western Europe and eastern America by 0.7 – 1 and 0.9 – 1.4 $\text{W}\cdot\text{m}^{-2}$ decade⁻¹ and decrease over India by -1 to -1.6 $\text{W}\cdot\text{m}^{-2}$ decade⁻¹ during the period 2001–2015. This is in line with the fact that even though concentration of aerosols is seen to be decreasing in eastern America, central South America, Europe and north-east of Oceania, it is increasing in the rest of the world (Mao *et al.*, 2014). Regionally, increase in aerosol burden and changes in their emission pattern is mostly attributed to anthropogenic activities (Dey and Girolamo, 2011; Babu

et al., 2013; Moorthy *et al.*, 2013; Kahn and Gaitley, 2015; Nair *et al.*, 2016; Srivastava, 2017; Zhao *et al.*, 2017). This is modulated further by the prevalent changes in meteorological parameters effectively enhancing the aerosol concentrations in the atmosphere (Yang *et al.*, 2016). Thus, the change in DRFs is highly dependent on the aerosol types in addition to columnar abundance. For example, black carbon (BC) imparts larger positive effect (Bond *et al.*, 2013; Zarzycki and Bond, 2010; Chung, 2012; Gogoi *et al.*, 2017). Similarly, SO_4 and OC cause larger negative effect (Collins *et al.*, 2002; Myhre *et al.*, 2013; Paulot *et al.*, 2018). Hence, trend analysis of DRFs itself is vital to estimate the change in radiative impact of aerosols. However, the global estimation of DRFs at different levels of the atmosphere that is, SFC, ATM and TOA is complex.

In the present study, the global distribution of DRFs and trends are uniquely studied using Clouds and Earth's Radiant Energy System (CERES; Wielicki *et al.*, 1996) Synoptic (SYN) climate quality daily data sets. CERES_SYN1deg solar and longwave downwelling surface fluxes were evaluated against measurements at 85 land and ocean sites around the globe over the period from March 2000 to December 2007, revealing a monthly mean bias of 2.2 $\text{W}\cdot\text{m}^{-2}$ (1.1%) for the shortwave and -4.1 $\text{W}\cdot\text{m}^{-2}$ (-1.2%) for the longwave irradiances (Rutan *et al.*, 2015). Moreover, CERES Science Team has applied the table of scaling factors for both Terra and Aqua to the observed TOA SW fluxes for the tuning of the computed fluxes. Thus, the synoptic data quality used in the present study is highly accurate and estimation of DRF over both regional and global scale at distinct atmospheric levels (i.e., SFC, ATM and TOA) adheres to improved estimation due to applications of updated CERES data sets. Based on this, the estimation of DRF and its trend in distinct geographical regions of the globe are themselves unique. The methodology adopted in the present study also serves as a primary proxy to accurately estimate global change in DRFs which is otherwise difficult to obtain from the limited in-situ measurements and high-computation modeling. Another important aspect in the present study is the long-term data base (2002–2017) chosen to examine the regional changes in aerosol loading in recent years over different parts of the globe. Thus, the estimation of DRF trends in the global scale in our study gives insight in to the identification of regional impact of aerosols on the Earth's energy budget associating distinct regional changes (increase/decrease).

2 | DATA AND METHODOLOGY

Daily global radiation data (CERES_SYN1deg-Day_Terra-Aqua-MODIS_Ed3A; Doelling *et al.*, 2013) measured by

CERES operating on-board Terra and Aqua satellite have been used to estimate the clear sky DRF at the TOA, ATM and SFC. The surface net radiations are estimated using the radiative transfer model with the atmospheric and surface properties obtained from MODIS, 3-hr geostationary (GEO) data and meteorological assimilation data from Goddard Earth Observation System (GEOS), while constraining both solar reflected and earth-emitted radiation for the TOA for all-sky and clear-sky conditions. Here, the radiative transfer calculation is made using the NASA Langley Research Center-Modified (LaRC) Fu-Liou radiative transfer model (Fu and Liou, 1993; Randles *et al.*, 2013; Rose *et al.*, 2013). The model is based on Fu-Liou scheme (Fu and Liou, 1992, 1993). This code is a modified version of the original Fu-Liou code to improve treatment of Rayleigh scattering and updated shortwave (SW) and longwave (LW) gaseous absorption (Kato *et al.*, 1999; Kratz and Rose, 1999). These computations use MODIS and geostationary cloud properties along with the atmospheric profiles of pressure, specific humidity and air temperature provided by NASA Global Modeling and Assimilation Office (GMAO; Reichle *et al.*, 2009) reanalyzes as inputs. Furthermore, the absorption by water vapor, carbon dioxide, methane and oxygen are treated using the methodology followed by Kato *et al.* (1999). The computations are constrained by the observed CERES TOA fluxes (Rutan *et al.*, 2015; Wang *et al.*, 2017). The model is further constrained by the aerosol optical depth and scattering properties for the vertical column from the Model for Atmospheric Transport and Chemistry (MATCH; Gidhagen *et al.*, 2005). The MATCH simulated aerosol properties are constrained by the observations from MODIS (Collins *et al.*, 2001; Levy *et al.*, 2013). The four modes of fluxes are used: pristine (clear, no-aerosols) and clear sky (clear, with aerosols) conditions at SFC and TOA. Here, ‘clear’ indicates ‘cloud free aerosol skies’. The aerosol forcing at TOA (DRF_{TOA}) and surface (DRF_{SFC}) is estimated by differencing net clear sky from net pristine sky fluxes and in the atmosphere (DRF_{ATM}) by subtracting the two DRFs as follows:

$$DRF_{TOA,SFC} = (F \downarrow \uparrow_{clear})_{TOA,SFC} - (F \downarrow \uparrow_{pristine})_{TOA,SFC} \quad (1)$$

$$DRF_{ATM} = DRF_{TOA} - DRF_{SFC} \quad (2)$$

Using long-term values of DRF at TOA, ATM and SFC, trends have been estimated. The Mann–Kendall test (Kendall, 1975, Li *et al.*, 2014; Mann, 1945) has been used to identify significance of the changes at the 95% confidence level.

The MODIS on-board Terra and Aqua satellites provides aerosol retrievals over both land and ocean that are

suitable for studying regional distribution of aerosol sources and trends. In this study, MODIS derived Aerosol optical depth (AOD, τ_λ), and Angstrom exponent (α) are used to understand aerosol loading and information on aerosol size distribution in the atmosphere. While AOD is the integrated extinction coefficient over columns of unit cross section measured at a particular wavelength (λ), values of given information on aerosol size distribution in the atmosphere. Following Angstrom (1929), α is estimated as:

$$\alpha = \frac{\log \frac{\tau_{\lambda_1}}{\tau_{\lambda_2}}}{\log \frac{\lambda_2}{\lambda_1}} \quad (3)$$

where, τ_{λ_1} and τ_{λ_2} are AOD at wavelength λ_1 and λ_2 , respectively.

α is inversely related with the particle size, that is, $\alpha \leq 1$ indicates size distribution dominated by coarse mode aerosols and $\alpha \geq 1$ by fine mode aerosols.

In addition, present study uses columnar SO_2 retrieved from OMI onboard Aqua satellite (Fioletov *et al.*, 2013; Krotkov *et al.*, 2016) for the period 2004–2017. OMI is the result of a partnership between NASA and the Dutch and Finnish meteorological institutes and space agencies flying on the NASA EOS Aura satellite (Levelt *et al.*, 2006; Schoeberl *et al.*, 2006). The OMI SO_2 product uses spectral measurements between 310.5 and 340.0 nm in the UV-2 (Li *et al.*, 2013).

3 | RESULTS AND DISCUSSIONS

3.1 | Global distribution of aerosol DRF

The global distribution of aerosol DRF shows (Figure 1) highly heterogeneous properties, having significant region-specific temporal change in absolute magnitude from 2001 to 2017. The global average DRF_{TOA} and DRF_{SFC} during the observational period (2001–2017) are $-5.36 \pm 0.04 \text{ W}\cdot\text{m}^{-2}$ and $-9.64 \pm 0.07 \text{ W}\cdot\text{m}^{-2}$, respectively, along with an atmospheric warming of $4.27 \pm 0.04 \text{ W}\cdot\text{m}^{-2}$. Magnitudes of temporal changes in DRFs are found to be higher over most of the continental hotspots of the Northern Hemisphere, where the source of strong aerosol emission exists. Average (during 2001–2017) DRF_{TOA}/DRF_{SFC} over the land alone is $-5.72 \pm 0.04 \text{ W}\cdot\text{m}^{-2}/-13.71 \pm 0.11 \text{ W}\cdot\text{m}^{-2}$ which translates to atmospheric warming of $7.99 \pm 0.07 \text{ W}\cdot\text{m}^{-2}$. During 2001, average values of the global DRF_{TOA} and DRF_{SFC} over land are -5.93 and $-13.8 \text{ W}\cdot\text{m}^{-2}$, resulting to atmospheric warming of $7.87 \text{ W}\cdot\text{m}^{-2}$. This is close to that reported earlier by Patadia *et al.* (2008), where, the

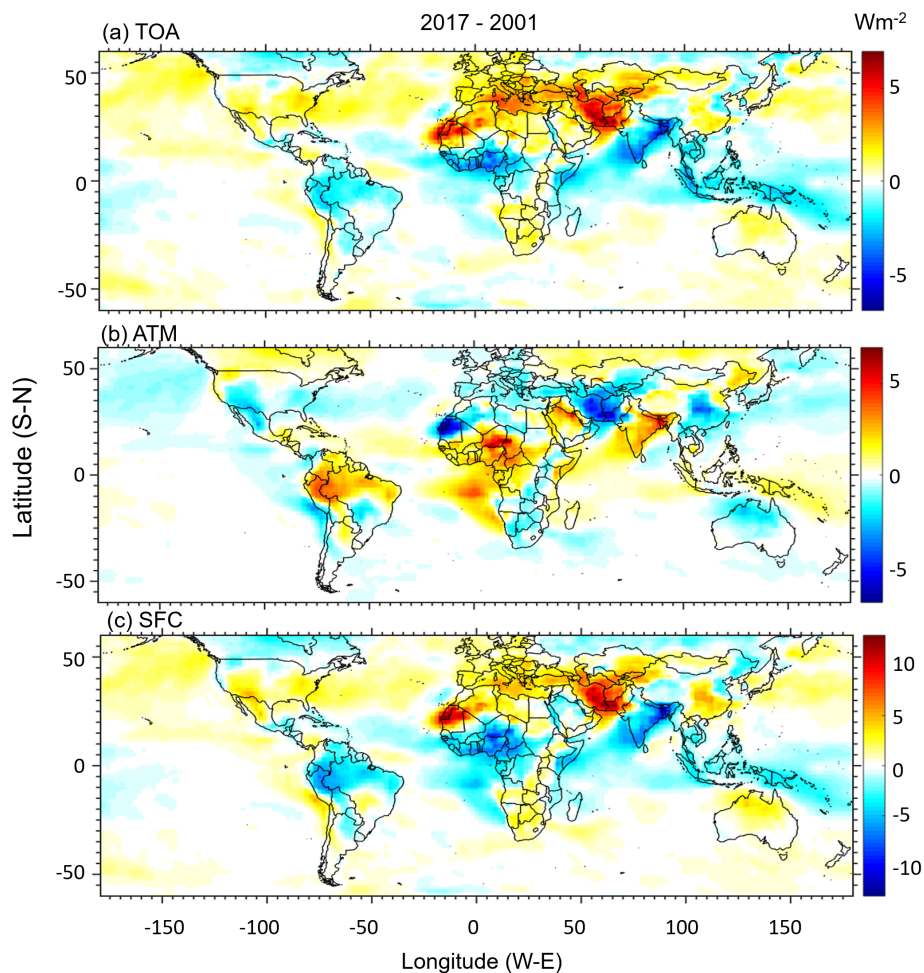


FIGURE 1 The difference in aerosol direct radiative forcing between 2017 and 2001 at the top of the atmosphere (a, TOA), in the atmosphere (b, ATM) and at the surface (c, SFC) as obtained from CERES synoptic (SYN) 1° datasets over the globe. Global distribution of aerosol direct radiative forcing during the respective years of 2001 and 2017 are shown in Figure S1

DRF_{TOA} was found to be $-5.1 \text{ W}\cdot\text{m}^{-2}$ (2000–2001) over the land. Compared to 2001, global land DRF_{TOA} is altered by $\sim 3.6\%$ in 2017, where, the magnitudes of DRF_{TOA} , DRF_{SFC} and DRF_{ATM} reach -5.72 , -13.77 and $8.05 \text{ W}\cdot\text{m}^{-2}$ during the later year. It is interesting to note that the geographic regions of Africa, south and east Asia consistently show higher values of DRFs during both the years: 2001 and 2017 (Figure S1). Collins *et al.* (2002) have reported that the surface insolation (under cloud free skies) over the Indian sub-continent is reduced by $40 \text{ W}\cdot\text{m}^{-2}$ during spring (1999) due to the impact of natural and anthropogenic aerosols, accompanied by warming ($25 \text{ W}\cdot\text{m}^{-2}$) in the atmosphere. In the present study, the values of DRF_{ATM} over the highly polluted Indo-Gangetic Plains (IGP) is as high as $\sim 30 \text{ W}\cdot\text{m}^{-2}$ during 2017, along with a reduction in the surface reaching flux by about $45 \text{ W}\cdot\text{m}^{-2}$. East China shows higher surface dimming in the beginning of the study period which reduces during the later years. DRF_{TOA} over Africa is comparatively low ($\sim -12 \text{ W}\cdot\text{m}^{-2}$) during both the years, but the DRF_{SFC} and DRF_{ATM} extend to -40 and $30 \text{ W}\cdot\text{m}^{-2}$, respectively. Rest of the land area experiences much lower values of DRF.

On the other hand, oceanic regions exhibit lower perturbation of the solar radiation due to lower aerosol loading, inferring an average value of $2.99 \pm 0.04 \text{ W}\cdot\text{m}^{-2}$ in the atmosphere associated with the cooling at the TOA by $-5.24 \pm 0.04 \text{ W}\cdot\text{m}^{-2}$ and surface dimming of $-8.23 \pm 0.07 \text{ W}\cdot\text{m}^{-2}$ (averaged from 2001 to 2017). Values of DRFs are higher near the west coast of Africa and east coast of Asia, similar to that reported by Zhang *et al.* (2005) where DRF ($-5.3 \text{ W}\cdot\text{m}^{-2}$) was estimated over cloud-free global oceans using the collocated MODIS and CERES data for the period November 2000–August 2001. Oceanic DRF_{TOA} , DRF_{ATM} and DRF_{SFC} (-5.25 , 2.94 and $-8.19 \text{ W}\cdot\text{m}^{-2}$, respectively) in 2001 was changed by 1.9 , 1.4 and 1.7% (-5.15 , 2.90 and $-8.05 \text{ W}\cdot\text{m}^{-2}$), respectively in 2017. These changes are much lower compared to that of the land. Anthropogenic aerosols are found to contribute significantly on the total aerosol loading over the oceanic region predominantly over the regions where the values of DRFs are found higher (Boucher and Haywood, 2001; Bellouin *et al.*, 2005; Li *et al.*, 2014). Strong dust plumes originating from Asia reaches northern Pacific Ocean and west coast of North America. These regions exhibit annual DRF_{SFC} of $\sim -14 \text{ W}\cdot\text{m}^{-2}$ and DRF_{ATM} of

$\sim 8 \text{ W}\cdot\text{m}^{-2}$ during 2001 (similar to Zhang *et al.*, 2005). Fire activities are persistent near the west and east coast of South America resulting to atmospheric forcing of $\sim 12 \text{ W}\cdot\text{m}^{-2}$. The aerosol forcing has a strong seasonal and regional dependence which are addressed in various studies in the past (Hatzianastassiou *et al.*, 2004; Quaas *et al.*, 2008; Randles and Ramaswamy, 2008; Pathak *et al.*, 2016; Nair *et al.*, 2016; Paulot *et al.*, 2018; Subba *et al.*, 2018; Yang *et al.*, 2018) and is not the primary focus of this study.

3.2 | Trends in global aerosol direct radiative forcing

The above results clearly indicate that in recent years, there has been potential change of the radiative balance of the atmosphere due to the impact of aerosols. Considering 2001 as base year, the DRF_{TOA} , DRF_{ATM} and DRF_{SFC} trend over the globe are found to be 0.02, -0.02 , and $0.03 \text{ W}\cdot\text{m}^{-2}\cdot\text{year}^{-1}$, respectively (Figure 2). The global land area exhibits rapid change of atmospheric forcing by $-0.03 \text{ W}\cdot\text{m}^{-2}\cdot\text{year}^{-1}$ associated with an increase in DRF_{TOA} and DRF_{SFC} by 0.02 and $0.05 \text{ W}\cdot\text{m}^{-2}\cdot\text{year}^{-1}$. However, oceanic region shows relatively weaker change in the DRF trend which is consistent with the comparatively lower change in the underlying oceanic surface and aerosol loading over majority of oceanic region. General trend in atmospheric forcing and surface dimming over oceanic regions is -0.01 and $0.03 \text{ W}\cdot\text{m}^{-2}\cdot\text{year}^{-1}$, respectively, almost half of the values over land regions.

Over land regions, trend of DRF_{TOA} are decreasing mostly over eastern and western of Africa, and south Asia, as against slightly increasing trend seen over North America and Europe (Figure 3). There cannot be one to one correlation between the radiative effect and the aerosols over every region. Especially over India, east and central China, South America, Africa due to the heterogeneity in the aerosol type (Paulot *et al.*, 2018). Anthropogenic emissions over India and China are expected to be more uncertain than those over America and Europe (Pan *et al.*, 2015; Saikawa *et al.*, 2017). For example, India has been experiencing changes in surface albedo due to underlying surface properties (Paulot *et al.*, 2018). Increase in rainfall and decrease in dust emissions (Pandey *et al.*, 2017) have caused more greening over the north-western regions (Jin and Wang, 2018). The decrease in surface albedo over India masks the effect of the increasing anthropogenic emissions on the outgoing radiation (Paulot *et al.*, 2018). This can change the signs of TOA forcing (Satheesh, 2002).

Since, aerosol forcing is dependent on the regional heterogeneity of land surface and aerosol loading, we have selected six distinct regions (R1-R6; R1- North-East America,

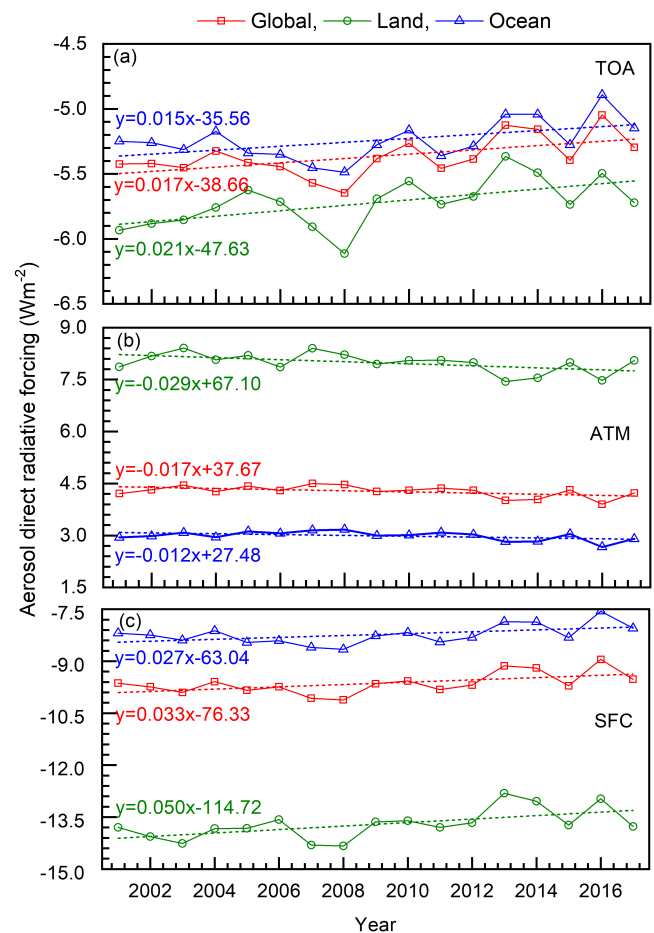


FIGURE 2 The trend in clear-sky shortwave aerosol direct radiative forcing (a) at the top of the atmosphere (TOA), (b) in the atmosphere (ATM) and (c) at the surface (SFC), averaged over the entire globe, global land and oceanic regions

R2- South America, R3-Europe, R4-Africa and Middle East countries, R5-south Asia and R6- eastern China) having significant trends and greater influence in overall DRFs. The trend of DRFs over each of these regions reveals substantial changes (Figure 3, Table 1). These changes are much greater than that of the global averaged changes, indicating the heterogeneous spread of aerosols. Trend over R2 and R4 are least ($\text{DRF}_{\text{TOA}} < 0.012 \text{ W}\cdot\text{m}^{-2}\cdot\text{year}^{-1}$), while showing weak increasing trends over R1, R3 and R6 (0.074 , 0.114 and $0.038 \text{ W}\cdot\text{m}^{-2}\cdot\text{year}^{-1}$). However, DRF trend over R5 is unique indicating decreasing trend of TOA cooling ($-0.076 \text{ W}\cdot\text{m}^{-2}\cdot\text{year}^{-1}$) and increasing trend of ATM warming ($0.025 \text{ W}\cdot\text{m}^{-2}\cdot\text{year}^{-1}$). These changes can be attributed to change in both mass loading and type of aerosols over these regions. Decreasing trend of cooling at TOA is attributed to increase in the fraction of absorbing AOD and decrease in aerosol single scattering albedo, respectively. Growth in the small sized particles, mostly of anthropogenic origin enhancing the cooling at the TOA. These properties are discussed in the following section.

3.3 | Regional variability of DRF

The long-term change in DRFs indicate that there has been profound change in aerosol burden across the globe in recent decades. We find potential enhancement of

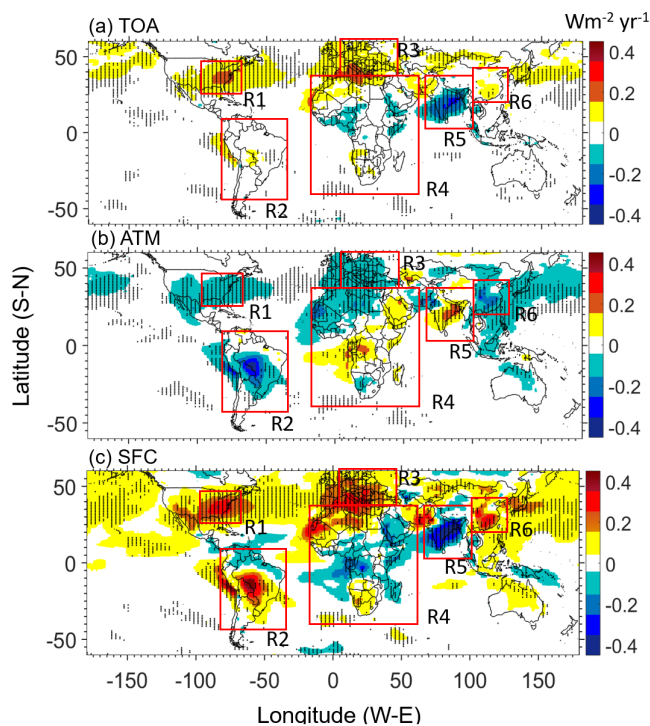


FIGURE 3 The global distribution of trend in clear-sky shortwave aerosol direct radiative forcing (a) at the top of the atmosphere (TOA), (b) in the atmosphere (ATM) and (c) at the surface (SFC). The red boxes represent distinct geographic regions denoted by R1–R6. Dotted areas are regions having significant trend above the 95% confidence level

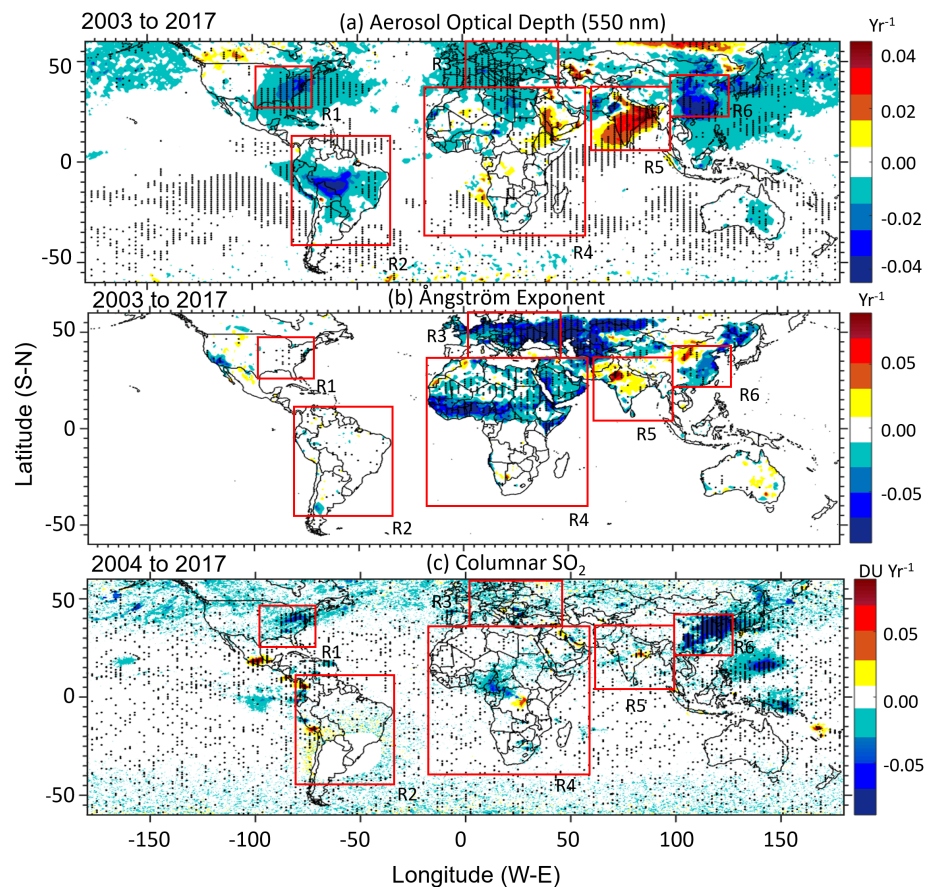
atmospheric warming ($>0.04 \text{ W}\cdot\text{m}^{-2}\cdot\text{year}^{-1}$) over central, eastern IGP and southern India, southern and central part of Africa and Middle East countries and their adjacent water bodies. Rest of the globe shows the opposite. To understand the behavior of aerosols, we have investigated the spatio-temporal distributions of aerosol optical depth (AOD) and Ångström exponent (α) obtained from MODIS onboard Terra and Aqua satellites. Since the change in the DRFs in the recent decade is mostly attributed to the anthropogenic emissions, we have also studied the change in columnar SO_2 retrieved from OMI onboard Aqua satellite (Fioletov *et al.*, 2013; Krotkov *et al.*, 2016). Although SO_2 is just one of the precursor gases of the sulfate aerosol and not always the representative of the anthropogenic aerosols, we have examined its global distribution and trends to understand the widespread emissions by fossil fuel combustion, which is a major source of anthropogenic aerosols. We see that there have been significant positive trends of AOD over the continental regions, such as central and eastern parts of the IGP (R5), Middle East countries and the central part of Africa (R4), along with their adjacent water bodies such as the Arabian Sea, the northern Bay-of-Bengal and the east coast of Africa (Figure 4a). Whereas, continental regions such as eastern parts of the United States, South America, European countries, eastern China and their adjacent water bodies show negative trends in AOD (-0.01 to $-0.04 \text{ AOD}\cdot\text{year}^{-1}$). In line with this, the values of α (a qualitative indicator of the size of aerosol particles following the inverse relationship [Ångström, 1929]; higher values indicate fine mode particles and vice versa) also exhibits significant changes over the period 2003–2017; especially over eastern China, India, Europe, the Middle East countries and Africa (Figure 4b).

TABLE 1 The values of DRFs at top of the atmosphere (TOA), surface (SFC) and in the atmosphere (ATM) in 2001, 2017 and their respective trends during the period 2001–2017 over the globe, land, ocean, region R1–R6

Regions	DRF in 2001 ($\text{W}\cdot\text{m}^{-2}$)			DRF in 2017 ($\text{W}\cdot\text{m}^{-2}$)			DRF trend ($\text{W}\cdot\text{m}^{-2}\cdot\text{year}^{-1}$)		
	TOA	ATM	SFC	TOA	ATM	SFC	TOA	ATM	SFC
GLOBE	−5.4	4.2	−9.6	−5.3	4.2	−9.5	0.017	−0.017	0.033
LAND	−5.9	7.9	−13.8	−5.7	8.1	−13.8	0.021	−0.029	0.050
OCEAN	−5.2	2.9	−8.2	−5.1	2.9	−8.0	0.015	−0.012	0.027
R1 (Northeast America)	−6.4	5.2	−11.6	−5.9	5.0	−10.9	0.074	−0.053	0.127
R2 (South America)	−4.7	6.8	−11.5	−5.2	7.4	−12.6	0.012	−0.065	0.077
R3 (Europe)	−8.7	7.5	−16.3	−7.0	7.1	−14.1	0.114	−0.076	0.191
R4 (Africa and Middle East countries)	−7.1	8.5	−15.6	−7.0	8.9	−15.9	0.001	0.002	−0.001
R5 (South Asia)	−9.7	9.7	−19.4	−10.7	10.4	−21.0	−0.076	0.025	−0.102
R6 (Eastern China)	−8.8	8.3	−17.2	−8.7	8.0	−16.7	0.038	−0.060	0.102

Note: The statistical significance of the trends is determined by the Mann–Kendall test.

FIGURE 4 The trends of (a) aerosol optical depth (AOD) at 550 nm, (b) angstrom exponent and (c) columnar sulfur dioxide (SO_2). Dotted areas are the regions having significant trend above the 95% confidence level. The red box represents different regions R1–R6



This reveals that not only the amount of global aerosol loading has changed; simultaneously the physico-chemical properties of aerosols have also been changed. However, change in total columnar AOD is not just caused evenly by the change in the amounts of all types of aerosols, but is rather driven by the predominant contributors of the composite aerosols. This can be observed in terms of the change of α , which especially increase over the Indian subcontinent and central China. This is attributed to increasing anthropogenic activities in response to growing population and urbanization resulting in higher emission of small sized particles. Various studies in the past have shown that the aerosol loading over the Indian subcontinent is highly influenced by the anthropogenic aerosol loading/activities over the region (Babu *et al.*, 2013; Moorthy *et al.*, 2013; Srivastava *et al.*, 2017; Pathak *et al.*, 2016). SO_2 is one of the major precursors of the anthropogenic aerosols (Smith *et al.*, 2011) and falls within the sub-micron range. Investigation of long-term SO_2 indicates that the increase in α coincides with the increase in SO_2 loadings (Figure 4c) over eastern IGP, whereas other parts of the Indian subcontinent (region R5) do not show similar variation of SO_2 and α . Similarly, the positive trend of SO_2 over the boundary of Peru and Chile (region R2) and central Africa (Republic of Congo;

region R4) is not consistent with the collocated positive trend of α . In contrast, eastern China (R6) shows decline in aerosol loading and corresponding decline in columnar SO_2 ($-0.08 \text{ DU} \cdot \text{year}^{-1}$). Recently, reported similar decline in SO_2 values (2004–2016). Similarly, a small region of Africa, middle east and south America (Figure 4c) show increase in SO_2 , where α also shows an increasing trend. Thus, the increasing/decreasing trend of AOD (Figure 4a) seen over distinct regions of the globe can be attributed to various factors (e.g., varying source processes and transport pathways, etc.). Over the Indian region, very good association between the increasing trends of AOD and SO_2 over the eastern IGP indicates the growing role of anthropogenic activities over this region, while the rest of country experiences the influence of the aerosol loading which are driven by various other sources. These include the emissions from thermal power plants, industrial, residential, transportation and commercial divisions, constructional areas, livestock farming and fertilizer applications, biomass burning, wild forest fires, desert dust plumes, marine aerosols and biogenic emissions, etc. (IPCC, 2007; IPCC, 2013; Dey and Girolamo, 2011; Streets *et al.*, 2013; Benedetti *et al.*, 2014; Matthias *et al.*, 2018). Among these, emissions of dust, sulfate and organic carbon enhancing their abundance in

the troposphere is significant (Fadnavis *et al.*, 2019) in altering the incoming solar radiation. The western part of India, where dust is the primary contributor of aerosol loading, exhibits decreasing trend of DRF_{SFC} driven by decreasing trend of dust aerosols in the last decade (Pandey *et al.*, 2017). Similarly, contributions of carbonaceous components to the long-term trend of DRF over the Indian region cannot be ignored. From the study of BC trend over the Indian region, Manoj *et al.* (2019) have indicated the presence of carbonaceous aerosols in the elevated lower free-tropospheric regions, even though a general decreasing trend of BC near the surface was revealed from the study.

In addition to distinct source processes, influence of regional climate variables (e.g., seasonal and regional rainfall) on the variability of aerosol loading is important. Babu *et al.* (2013) have shown that increasing trend in AOD over the IGP can be attributed to the competing effects of aerosol influx and reduced wet removal impact of aerosols. Thus, the sharp increase in atmospheric warming over the Indian sub-continent can be attributed to the complex interaction between natural and anthropogenic forcing at different spatio-temporal scales, modulated by regional climate variables.

Based on the above observations, increasing trend in TOA cooling can be synchronous with the change in anthropogenic aerosol loading, where the emission of SO_2 hold significance over eastern America, parts of Africa and eastern China and the adjoining oceanic region. Zhao *et al.* (2017) attributed the decreasing trend of DRFs over eastern United States and Europe to decrease in SO_2 and NO_x which are the precursors for the secondary aerosol formations, except for mineral dust and ammonia especially after 2011. Similarly, 25–50% of organic carbon (30% of PM) over US was found to decline between 1990 and 2012, with no significant change in biogenic aerosols (Ridley 2018; Blanchard *et al.*, 2013, 2016; Attwood *et al.*, 2014). This is attributed to decline in the anthropogenic emissions predominantly from vehicular and residential fuel burning related to series of control measurements under the Clean Air Act (Xing *et al.*, 2013).

Interestingly, R1 exhibits increasing trend until 2007 (DRF_{ATM} trend: $0.13 \text{ W}\cdot\text{m}^{-2}\cdot\text{year}^{-1}$) and a decreasing trend after 2007 (DRF_{ATM} trend: $-0.15 \text{ W}\cdot\text{m}^{-2}\cdot\text{year}^{-1}$). Similar bimodal trend was observed by Paulot *et al.* (2018) over the same region. Decrease in DRFs is indicative of the positive result of the implementation of various air pollution acts (Wang *et al.*, 2014). However, it is important to note that though there has been decrease in DRFs over East China (Figure 2), their magnitudes in the recent years are still higher over some of the locations compared to the rest of the world (Figure 1 and Figure 2). Hence, continuous mitigation of air quality is still important.

4 | CONCLUSIONS

Present study demonstrates an extensive utilization of the combination of space-borne radiation flux measurements and radiative transfer modeling for improved quantitative estimation of global aerosol DRF trend over the period from 2001 to 2017. Since there exist noticeable discrepancies in the estimation of aerosol trends from various satellite retrievals (e.g., MODIS, MISR, OMI), most likely due to the difference in spatio-temporal sampling, observing strategy and retrieval algorithms (Kahn *et al.*, 2009; Zhao *et al.*, 2017), consideration of direct radiation measurements by satellite sensor is unique and suitable for global radiation budget studies. Thus, utilization of highly accurate synoptic (SYN) datasets from Clouds and Earth's Radiant Energy System (CERES) provides updated information on the global distribution of DRF trend, which is otherwise difficult to obtain from the limited in-situ measurements and high-computation modeling. The major outcomes of this study include:

1. In the recent decades, there have been substantial changes in the regional and global distribution of DRFs due to aerosols. The global (-60°S to 60°N) values indicate a decreasing trend of TOA forcing (i.e., a reduced cooling effect) by $0.017 \text{ W}\cdot\text{m}^{-2}\cdot\text{year}^{-1}$, along with a decreasing trend of atmospheric forcing (i.e., a reduced warming effect) by $-0.017 \text{ W}\cdot\text{m}^{-2}\cdot\text{year}^{-1}$ having rapid change over the land ($-0.029 \text{ W}\cdot\text{m}^{-2}\cdot\text{year}^{-1}$) compared to that over the ocean ($-0.012 \text{ W}\cdot\text{m}^{-2}\cdot\text{year}^{-1}$). While many distinct geographic regions (over land) of the globe depicted a general decreasing trend of the atmospheric forcing (warming) ranging from $-0.053 \text{ W}\cdot\text{m}^{-2}\cdot\text{year}^{-1}$ in North-east America to $-0.076 \text{ W}\cdot\text{m}^{-2}\cdot\text{year}^{-1}$ in Western Europe, Africa and South Asia showed increasing trend (i.e., an enhanced warming effect in the atmosphere) by $0.002 \text{ W}\cdot\text{m}^{-2}\cdot\text{year}^{-1}$ and $0.025 \text{ W}\cdot\text{m}^{-2}\cdot\text{year}^{-1}$ respectively.

2. Global map of AOD reveal significant positive trend over the continental regions, such as central and east Indo-Gangetic basins of India, Middle East countries and Africa, along with their adjacent water bodies such as Arabian Sea, North Bay of Bengal and east coast of Africa.

3. The global trend of DRF can be attributed largely to the anthropogenic aerosols. The increasing trend of SO_2 over eastern IGP, a small region of Africa, Middle East, and South America indicates increase in anthropogenic activities over these regions and may be a dominant factor in governing the DRF trend over these regions.

ACKNOWLEDGEMENT

This work was carried out as part of the Aerosol Radiative Forcing over India (ARFI) project of ISRO-GBP. The authors thank CERES, OMI and MODIS science team for

providing scientific datasets, which have been obtained through the NASA Langley Distributed Active Archive Systems and GIOVANNI portal. Tamanna Subba was supported by ARFI project fellowship from ISRO-GBP and Kalam-Climate Doctoral Fulbright Fellowship program 2017–2018 under USIEF. Binita Pathak is a junior associate of ICTP, Italy.

ORCID

Tamanna Subba  <https://orcid.org/0000-0002-0319-9751>

Mukunda M. Gogoi  <https://orcid.org/0000-0003-1008-911X>

Pradip K. Bhuyan  <https://orcid.org/0000-0001-7619-847X>

REFERENCES

- Aas, W., Mortier, A., Bowersox, V., Cherian, R., Faluvegi, G., Fagerli, H., Hand, J., Klimont, Z., Galy-Lacaux, C., Lehmann, C.M.B., Myhre, C.L., Myhre, G., Olivié, D., Sato, K., Quaas, J., Rao, P.S.P., Schulz, M., Shindell, D., Skeie, R.B., Stein, A., Takemura, T., Tsyro, S., Vet, R. and Xu, X. (2019) Global and regional trends of atmospheric sulfur. *Scientific Reports*, 9, 953. <https://doi.org/10.1038/s41598-018-37304-0>.
- Angstrom, A. (1929) On the atmospheric transmission of sun radiation and on dust in the air. *Geografiska Annaler*, 11, 156–166.
- Attwood, A.R., et al. (2014) Trends in sulfate and organic aerosol mass in the southeast U.S.: impact on aerosol optical depth and radiative forcing. *Geophysical Research Letters*, 41, 7701–7709.
- Babu, S.S., Manoj, M.R., Moorthy, K.K., Gogoi, M.M., Nair, V.S., Kompalli, S.K., Satheesh, S.K., Niranjana, K., Ramagopal, K., Bhuyan, P.K. and Singh, D. (2013) Trends in aerosol optical depth over Indian region: potential causes and impact indicators. *Journal of Geophysical Research*, 118, 1–13. <https://doi.org/10.1002/2013JD020507>.
- Bellouin, N., Boucher, O., Haywood, J. and Reddy, M.S. (2005) Global estimate of aerosol direct radiative forcing from satellite measurements. *Nature*, 438, 22–29. <https://doi.org/10.1038/nature04348>.
- Benedetti, A., Baldasano, J.M., Basart, S., Benincasa, F., Boucher, O., Brooks, M.E., Chen, J.-P., Colarco, P.R., Gong, S., Huneeus, N., Jones, L., Lu, S., Menut, L., Morcrette, J.-J., Mulcahy, J., Nickovic, S., Pérez García-Pando, C., Reid, J.S., Sekiyama, T.T., Tanaka, T.Y., Terradellas, E., Westphal, D.L., Zhang, X.-Y. and Zhou, C.-H. (2014) Operational dust prediction. In: *Mineral Dust*. Dordrecht: Springer, pp. 223–265.
- Blanchard, C.L., Hidy, G.M., Shaw, S., Baumann, K. and Edgerton, E.S. (2016) Effects of emission reductions on organic aerosol in the southeastern United States. *Atmospheric Chemistry Physics*, 16, 215–238.
- Blanchard, C.L., Hidy, G.M., Tanenbaum, S., Edgerton, E.S. and Hartsell, B.E. (2013) The southeastern aerosol research and characterization (SEARCH) study: temporal trends in gas and PM concentrations and composition, 1999–2010. *Journal of the Air & Waste Management Association*, 63, 247–259.
- Bond, T.C., Doherty, S.J., Fahey, D.W., Forster, P.M., Berntsen, T., DeAngelo, B.J., Flanner, M.G., Ghan, S., Karcher, B., Koch, D., Kinne, S., Kondo, Y., Quinn, P.K., Sarofim, M.C., Schultz, M.G., Schulz, M., Venkataraman, C., Zhang, H., Zhang, S., Bellouin, N., Guttikunda, S.K., Hopke, P.K., Jacobson, M.Z., Kaiser, J.W., Klimont, Z., Lohmann, U., Schwarz, J.P., Shindell, D., Storelvmo, T., Warren, S.G. and Zender, C.S. (2013) Bounding the role of black carbon in the climate system: A scientific assessment. *Journal of Geophysical Research-Atmospheres*, 118, 5380–5552. <https://doi.org/10.1002/jgrd.50171>.
- Boucher, O. and Haywood, J. (2001) On summing the components of radiative forcing of climate change. *Climate Dynamics*, 18, 297–302.
- Christopher, S.A. and Zhang, J. (2004) Cloud-free shortwave aerosol radiative effect over oceans: strategies for identifying anthropogenic forcing from Terra satellite measurements. *Geophysical Research Letters*, 31, L18101. <https://doi.org/10.1029/2004GL020510>.
- Chung, C.E. (2012) Direct Radiative forcing: a review, atmospheric aerosols: regional characteristics. *Chemistry and Physics*, 1, 379–394. <https://doi.org/10.5772/50248>.
- Chung, C.E., Ramanathan, V., Kim, D. and Podgorny, I.A. (2005) Global anthropogenic aerosol direct forcing derived from satellite and ground-based observations. *Journal of Geophysical Research*, 110, D24207.
- Collins, W.D., et al. (2002) Simulation of aerosol distributions and radiative forcing for INDOEX: regional climate impacts. *Journal of Geophysical Research*, 107(D19), 8028, 1–20. <https://doi.org/10.1029/2000JD000032>.
- Collins, W.D., Rasch, P.J., Eaton, B.E., Khattatov, B.V., Lamarque, J.-F. and Zender, C.S. (2001) Simulating aerosols using a chemical transport model with assimilation of satellite aerosol retrievals: methodology for INDOEX. *Journal of Geophysical Research*, 106, 7313–7336.
- Contreras, R.R., Zhang, J., Reid, J.S. and Christopher, S. (2017) A study of 15-year aerosol optical thickness and direct shortwave aerosol radiative effect trends using MODIS, MISR, CALIOP and CERES. *Atmospheric Chemistry Physics*, 17, 13849–13868.
- Dey, S. and Girolamo, D.L. (2011) A decade of change in aerosol properties over the Indian subcontinent. *Geophysical Research Letters*, 38, L14811.
- Doelling, D.R., Loeb, N.G., Keyes, D.F., Nordeen, M.L., Morstad, D., Nguyen, C., Wielicki, B.A., Young, D.F. and Sun, M. (2013) Geostationary enhanced temporal interpolation for CERES flux products. *Journal of Atmospheric and Oceanic Technology*, 30, 1072–1090.
- Fadnavis, S., Sabin, T.P., Roy, C., Rowlinson, M., Rap, A., Vernier, J.P. and Sioris, C.E. (2019) Elevated aerosol layer over South Asia worsens the Indian droughts. *Scientific Reports*, 9, 10268. <https://doi.org/10.1038/s41598-019-46704-9>.
- Fioletov, V.E., et al. (2013) Application of OMI, SCIAMACHY, and GOME-2 satellite SO₂ retrievals for detection of large emission sources. *Journal of Geophysical Research*, 118, 11399–11418.
- Forster, P., Ramaswamy, V., Artaxo, P., Berntsen, T., Betts, R., Fahey, D.W., Haywood, J., Lean, J., Lowe, D.C., Myhre, G., Nganga, J., Prinn, R., Raga, G., Schulz, M. and Van Dorland, R. (2007) Changes in atmospheric constituents and in radiative forcing. Cambridge, UK: Cambridge University Press.
- Fu, Q. and Liou, K.N. (1992) On the correlated k-distribution method for radiative transfer in nonhomogeneous atmospheres. *Journal of the Atmospheric Sciences*, 49, 2139–2156.

- Fu, Q. and Liou, K.N. (1993) Parameterization of the radiative properties of cirrus clouds. *Journal of the Atmospheric Sciences*, 50, 2008–2025.
- Gogoi, M.M., Babu, S.S., Moorthy, K.K., Bhuyan, P.K., Pathak, B., Subba, T., Bharali, C., Chutia, L., Kundu, S.S., Borgahain, A., De, B.K., Guha, A. and Singh, S.B. (2017) *Radiative Effects of Absorbing Aerosols over Northeastern India: Observations and model simulations*. *Journal of Geophysical Research*. <https://doi.org/10.1002/2016JD025592>.
- Gidhagen, L., Johansson, C., Langner, J. and Foltescu, V.L. (2005) Urban scale modelling of particle number concentrations in Stockholm. *Atmospheric Environment*, 39, 1711–1725.
- Hansen, J., Sato, M., Lacis, A. and Ruedy, R. (1997) The missing climate forcing. *Phil. Trans. Royal Society. London B*, 352, 231–240.
- Hatzianastassiou, N., Katsoulis, B. and Vardavas, I. (2004) Global distribution of aerosol direct radiative forcing in the ultraviolet and visible arising under clear skies. *Tellus B: Chemical and Physical Meteorology*, 56(1), 51–71. <https://doi.org/10.3402/tellusb.v56i1.16400>.
- Intergovernmental Panel on Climate Change (IPCC). (2007) *Climate Change 2007*. Cambridge, UK and New York, NY: Cambridge University Press.
- IPCC. (2013) *Climate Change 2013, Working group I contribution to the fifth assessment report of the Intergovernmental Panel on Climate Change*. Cambridge, UK and New York, NY: Cambridge University press, Cambridge.
- Jin, Q. and Wang, C. (2018) The greening of northwest Indian sub-continent and reduction of dust abundance resulting from Indian summer monsoon revival. *Scientific Reports*, 8, 4573. <https://doi.org/10.1038/s41598-018-23055-5>.
- Kahn, R.A. and Gaitley, B.J. (2015) An analysis of global aerosol type as retrieved by MISR. *Journal of Geophysical Research*, 120, 4248–4281.
- Kahn, R.A. (2012) Reducing the uncertainties in direct aerosol radiative forcing. *Surveys in Geophysics*, 33, 701–721. <https://doi.org/10.1007/s10712-011-9153-z>.
- Kahn, R., Petzold, A., Wendisch, M., Bierwirth, E., Dinter, T., Esselborn, M., Fiebig, M., Heese, B., Knippertz, P., Müller, D., Schladitz, A. and von Hoyningen-Huene, W. (2009) Desert dust aerosol air mass mapping in the Western Sahara, using particle properties derived from space-based multi-angle imaging. *Tellus*, 61B, 239–251. <https://doi.org/10.1111/j.1600-0889.2008.00398>.
- Kahn, R.A., Gaitley, B.J., Martonchik, J.V., Diner, D.J., Crean, K.A. and Holben, B. (2005) Multiangle Imaging Spectroradiometer (MISR) global aerosol optical depth validation based on 2 years of coincident Aerosol Robotic Network (AERONET) observations. *Journal of Geophysical Research: Atmospheres*, 110, D10S04. <https://doi.org/10.1029/2004jd004706>.
- Kato, S., Ackerman, T., Mather, J. and Clothiaux, E. (1999) The k-distribution method and correlated-k approximation for a shortwave radiative transfer model. *Journal of Quantitative Spectroscopy & Radiative Transfer*, 62, 109–121.
- Kendall, M.G. (1975) *Rank Correlation Methods*, 4th edition. London: Charles Griffin.
- Kratz, D.P. and Rose, F.G. (1999) Accounting for molecular absorption within the spectral range of the CERES window channel. *Journal of Quantitative Spectroscopy & Radiative Transfer*, 61, 83–95.
- Krotkov, N.A., McLinden, C.A., Li, C., Lamsal, L.N., Celarier, E.A., Marchenko, S.V., Swartz, W.H., Bucsela, E.J., Joiner, J., Duncan, B.N., Boersma, K.F., Veefkind, J.P., Levelt, P.F., Fioletov, V.E., Dickerson, R.R., He, H., Lu, Z. and Streets, D.G. (2016) Aura OMI observations of regional SO₂ and NO₂ pollution changes from 2005 to 2015. *Atmospheric Chemistry Physics*, 16, 4605–4629. <https://doi.org/10.5194/acp-16-4605-2016>.
- Levelt, P.F., Van Den Oord, G.H.J., Dobber, M.R., Mälkki, A., Visser, H., De Vries, J., Stammes, P., Lundell, J.O.V. and Saari, H. (2006) The ozone monitoring instrument. *IEEE Transactions on Geoscience and Remote Sensing*, 44, 1093–1101.
- Levy, H., Horowitz, L.W., Schwarzkopf, M.D., Ming, Y., Golaz, J.C., Naik, V. and Ramaswamy, V. (2013) The roles of aerosol direct and indirect effects in past and future climate change. *Journal of Geophysical Research: Atmospheres*, 118, 4521–4532. <https://doi.org/10.1002/jgrd.50192>.
- Levy, R.C., Remer, L.A., Tanré, D., Mattoo, S., Kaufman, Y.J. (2009) Algorithm for remote sensing of tropospheric aerosol over dark targets from MODIS: collections 005 and 051: revision 2; Feb Product ID: MOD04/MYD04, 1-95.
- Li, C., Joiner, J., Krotkov, N.a. and Bhartia, P.K. (2013) A fast and sensitive new satellite SO₂ retrieval algorithm based on principal component analysis: application to the ozone monitoring instrument. *Geophysical Research Letters*, 40, 6314–6318. <https://doi.org/10.1002/2013GL058134>.
- Li, J., Carlson, B.E., Dubovik, O. and Lacis, A.A. (2014) Recent trends in aerosol optical properties derived from AERONET measurements. *Atmospheric Chemistry Physics*, 14, 12271–12289.
- Loeb, N.G. and Kato, S. (2002) Top-of-atmosphere direct radiative effect of aerosols from the clouds and the Earth's radiant energy system satellite instrument (CERES). *Journal of Climate*, 15, 1474–1484.
- Mann, H.B. (1945) Nonparametric tests against trend. *Econometrica*, 13, 245–259.
- Manoj, M.R., Satheesh, S.K., Moorthy, K.K., Gogoi, M.M. and Babu, S.S. (2019) Decreasing trend in black carbon aerosols over the Indian region. *Geophysical Research Letters*, 46(5), 2903–2910. <https://doi.org/10.1029/2018GL081666>.
- Mao, K.B., Ma, Y., Xia, L., Chen, W.Y., Shen, X.Y., He, T.J. and Xu, T.R. (2014) Global aerosol change in the last decade: an analysis based on MODIS data. *Atmospheric Environment*, 94, 680–686. <https://doi.org/10.1016/j.atmosenv.2014.04.053>.
- Matthias, V., Arndt, J.A., Aulinger, A., Bieser, J., Denier van der Gon, H., Kranenburg, R., Kuenen, J., Neumann, D., Pouliot, G. and Quante, M. (2018) Modeling emissions for three-dimensional atmospheric chemistry transport models. *Journal of the Air & Waste Management Association*, 68(8), 763–800. <https://doi.org/10.1080/10962247.2018.1424057>.
- Moorthy, K.K., Babu, S.S., Manoj, M.R. and Satheesh, S.K. (2013) Buildup of aerosols over the Indian region. *Geophysical Research Letters*, 40, 1011–1014. <https://doi.org/10.1002/GRL.50165>.
- Murphy, D.M. (2013) Little net clear-sky radiative forcing from recent regional redistribution of aerosols. *Nature Geoscience*, 6, 258–262. <https://doi.org/10.1038/ngeo1740>.
- Murphy, D.M. and Ravishankara, A.R. (2018) Trends and patterns in the contributions to cumulative radiative forcing from different regions

- of the world. *Proceedings of the National Academy of Sciences*, 115 (52), 113192–113197. <https://doi.org/10.1073/pnas.1813951115>.
- Myhre, G., Shindell, D., Bréon, F.-M., Collins, W., Fuglestedt, J., Huang, J., Koch, D., Lamarque, J.-F., Lee, D., Mendoza, B., Nakajima, T., Robock, A., Stephens, G., Takemura, T. and Zhang, H. (2013) Anthropogenic and natural radiative forcing. In: *Climate Change 2013. The Physical Science Basis, Contribution of Working Group I to the Fifth Assessment Report of the Intergovernmental Panel on Climate Change*. Cambridge, United Kingdom and New York, NY, USA: Cambridge University Press.
- Nair, V.N., Babu, S.S., Manoj, M.R., Moorthy, K.K. and Chin, M. (2016) Direct radiative effects of aerosols over South Asia from observations and modelling. *Climate Dynamics*, 49, 1411–1428. <https://doi.org/10.1007/s00382-016-3384-0>.
- Pan, X., Chin, M., Gautam, R., Bian, H., Kim, D., Colarco, P.R., Diehl, T.L., Bauer, S. and Bellouin, N. (2015) A multi-model evaluation of aerosols over South Asia: common problems and possible causes. *Atmospheric Chemistry Physics*, 15, 5903–5928. <https://doi.org/10.5194/acp15-5903-2015>.
- Pandey, S.K., Vinoj, V., Landu, K. and Babu, S.S. (2017) Declining pre-monsoon dust loading over South Asia: signature of a changing regional climate. *Scientific Reports*, 7, 16062. <https://doi.org/10.1038/s41598-017-16338-w>.
- Patadia, F., Gupta, P. and Christopher, S.A. (2008) First observational estimates of global clear sky shortwave aerosol direct radiative effect over land. *Geophysical Research Letters*, 35, L04810. <https://doi.org/10.1029/2007GL032314>.
- Pathak, B., Subba, T., Dahutia, P., Bhuyan, P.K., Moorthy, K.K., Gogoi, M.M., Babu, S.S., Chutia, L., Ajay, P., Biswas, J., Bharali, C., Borgohain, A., Dhar, P., Guha, A., De, B.K., Banik, T., Chakraborty, M., Kundu, S.S., Sudhakar, S. and Singh, S.B. (2016) Aerosol characteristics in north-East India using ARFINET spectral optical depth measurements. *Atmospheric Environment*, 125, 461–473. <https://doi.org/10.1016/j.atmosenv.2015.07.038>.
- Paulot, F., Paynter, D., Naik, V. and Horowitz, L.W. (2018) Changes in the aerosol direct radiative forcing from 2001 to 2015: observational constraints and regional mechanisms. *Atmospheric Chemistry Physics*, 18, 13265–13281. <https://doi.org/10.5194/acp-18-13265>.
- Penner, J.E., Charlson, R.J., Schwartz, S.E., Hales, J.M., Laulainen, N.S., Travis, L., Leifer, R., Novakov, T., Ogren, J. and Radke, L.F. (1994) Quantifying and minimizing uncertainty of climate forcing by anthropogenic aerosols. *Bulletin of the American Meteorological Society*, 75, 375–400.
- Putaud, J.P., Cavalli, F., Martins dos Santos, S. and Dell'Acqua, A. (2014) Long-term trends in aerosol optical characteristics in the Po Valley. *Atmospheric Chemistry Physics*, 14, 9129–9136.
- Quaas, J., Boucher, O., Bellouin, N. and Kinne, S. (2008) Satellite-based estimate of the direct and indirect aerosol climate forcing. *Journal of Geophysical Research*, 113, D05204. <https://doi.org/10.1029/2007JD008962>.
- Randles, C.A., Kinne, S., Myhre, G., Schulz, M., Stier, P., Fischer, J., Doppler, L., Highwood, E., Ryder, C., Harris, B., Huttunen, J., Ma, Y., Pinker, R.T., Mayer, B., Neubauer, D., Hittenberger, R., Oreopoulos, L., Lee, D., Pitari, G., di Genova, G., Quaas, J., Rose, F. G., Kato, S., Rumbold, S.T., Vardavas, I., Hatzianastassiou, N., Matsoukas, C., Yu, H., Zhang, F., Zhang, H. and Lu, P. (2013) Intercomparison of shortwave radiative transfer schemes in global aerosol modeling: results from the AeroCom Radiative transfer experiment. *Atmospheric Chemistry and Physics*, 13, 2347–2379.
- Randles, C.A. and Ramaswamy, V. (2008) Absorbing aerosols over Asia: a geophysical fluid dynamics laboratory general circulation model sensitivity study of model response to aerosol optical depth and aerosol absorption. *Journal of Geophysical Research*, 113, D21203. <https://doi.org/10.1029/2008JD010140>.
- Reichle, R.H., et al. (2009) Recent advances in land data assimilation at the NASA global modeling and assimilation office. In: Park, S. K. and Xu, L. (Eds.) *Data Assimilation for Atmospheric, Oceanic and Hydrologic Applications*. Berlin, Heidelberg: Springer.
- Remer, L.A., Kaufman, Y.J., Tanré, D., Mattoo, S., Chu, D.A., Martins, J.V., Li, R.R., Ichoku, C., Levy, R.C., Kleidman, R.G., Eck, T.F., Vermote, E. and Holben, B.N. (2005) The MODIS aerosol algorithm, products, and validation. *Journal of the Atmospheric Sciences*, 62(4), 947–973.
- Remer, L.A., Kleidman, R.G., Levy, R.C., Kaufman, Y.J., Tanré, D., Mattoo, S., Martins, J.V., Ichoku, C., Koren, I., Yu, H. and Holben, B. (2008) Global aerosol climatology from the MODIS satellite sensors. *Journal of Geophysical Research*, 113, D14S07. <https://doi.org/10.1029/2007JD009661>.
- Ridley, D.A., Heald, C.L., Ridley, K.J. and Kroll, J.H. (2018) Causes and consequences of decreasing atmospheric organic aerosol in the United States. *Proceedings of the National Academy of Sciences*, 115(2), 290–295. <https://doi.org/10.1073/pnas.1700387115>.
- Rose, F.G., Rutan, D.A., Charlock, T.P., Smith, G.L. and Kato, S. (2013) An algorithm for the constraining of radiative transfer calculations to CERES-observed broadband top-of-atmosphere irradiance. *Journal of Atmospheric and Oceanic Technology*, 30, 1091–1106.
- Rutan, D.A., Kato, S., Ssai, D.R.D., Rose, F.G., Nguyen, L.T., Cladwell, T.E. and Loeb, N.G. (2015) CERES synoptic product: methodology and validation of surface radiant flux. *Journal of Atmospheric and Oceanic Technology*, 32, 1121–1143. <https://doi.org/10.1175/jtech-d-14-00165.1>.
- Saikawa, E., Trail, M., Zhong, M., Wu, Q., Young, C.L., JanssensMaenhout, G., Klimont, Z., Wagner, F., Ichi Kurokawa, J., Nagpure, A.S. and Gurjar, B.R. (2017) Uncertainties in emissions estimates of greenhouse gases and air pollutants in India and their impacts on regional air quality. *Environmental Research Letters*, 12, 065002. <https://doi.org/10.1088/1748-9326/aa6cb4>.
- Samset, B.H., Stjern, C.W., Andrews, E., Kahn, R.A., Myhre, G., Schulz, M. and Schuster, G.L. (2018) Aerosol absorption: Progress towards global and regional constraints. *Current Climate Change Reports*, 4, 65–83. <https://doi.org/10.1007/s40641-018-0091-4>.
- Satheesh, S.K. (2002) Aerosol radiative forcing over land: effect of surface and cloud reflection. *Annales Geophysicae*, 20, 2105–2109.
- Schoeberl, M.R., Douglass, A.R., Hilsenrath, E., Bhartia, P.K., Beer, R., Waters, J.W., Gunson, M.R., Froidevaux, L., Gille, J.C., Barnett, J. J., Levelt, P.F. and DeCola, P. (2006) Overview of the EOS aura mission. *IEEE Transactions on Geoscience and Remote Sensing*, 44, 1066–1072. <https://doi.org/10.1109/TGRS.2005.861950>.
- Seinfeld, J.H. and Pandis, S.N. (2006) *Atmospheric Chemistry and Physics, from Air Pollution to Climate Change*. Hoboken, NJ: Wiley.
- Smith, S.J., van Aardenne, J., Klimont, Z., Andres, R., Volke, A.C. and Delgado, A.S. (2011) Anthropogenic sulfur dioxide emissions: 1850–2005. *Atmospheric Chemistry and Physics*, 11, 1101–1116.

- Stevens, B. (2015) Rethinking the lower bound on aerosol Radiative forcing. *Journal of Climate*, 28, 4794–4819. <https://doi.org/10.1175/JCLI-D-14-00656.1>.
- Srivastava, R. (2017) Trends in aerosol optical properties over South Asia. *International Journal of Climatology*, 37(1), 371–380. <https://doi.org/10.1002/joc.4710>.
- Streets, D.G., Canty, T., Carmichael, G.R., de Foy, B., Dickerson, R. R., Duncan, B.N., Edwards, D.P., Haynes, J.A., Henze, D.K., Houyoux, M.R., Jacobi, D.J., Krotkov, N.A., Lamsal, L.N., Liu, Y., Lu, Z.F., Martini, R.V., Pfister, G.G., Pinder, R.W., Salawitch, R.J. and Wechti, K.J. (2013) Emissions estimation from satellite retrievals: A review of current capability. *Atmospheric Environment*, 77, 1011–1042. <https://doi.org/10.1016/j.atmosenv.2013.05.051>.
- Stocker, T.F., Qin, D., Plattner, G.-K., Alexander, L.V., Allen, S.K., Bindoff, N.L., Bréon, F.-M., Church, J.A., Cubasch, U., Emori, S., Forster, P., Friedlingstein, P., Gillett, N., Gregory, J.M., Hartmann, D.L., Jansen, E., Kirtman, B., Knutti, R., Krishna Kumar, K., Lemke, P., Marotzke, J., Masson-Delmotte, V., Meehl, I.I., Mokhov, G.A., Piao, S., Ramaswamy, V., Randall, D., Rhein, M., Rojas, M., Sabine, C., Shindell, D., Talley, L.D., Vaughan, D.G. and Xie, S.-P. (2013) Technical summary. In: *Climate Change 2013: The Physical Science Basis. Contribution of Working Group I to the Fifth Assessment Report of the Intergovernmental Panel on Climate Change*. New York: Cambridge University Press, pp. 33–115. <https://doi.org/10.1017/CBO9781107415324.005>.
- Su, W., Liang, L., Doelling, D.R., Minnis, P., Duda, D.P., Khlopenkov, K.V., et al. (2018) Determining the shortwave radiative flux from earth polychromatic imaging camera. *Journal of Geophysical Research*, 123(11), 479–491. <https://doi.org/10.1029/2018JD029390>.
- Subba, T., Gogoi, M.M., Pathak, B., Ajay, P., Bhuyan, P.K. and Solmon, F. (2018) Assessment of 1D and 3D model simulated radiation flux based on surface measurements and estimation of aerosol forcing and their climatological aspects. *Atmospheric Research*, 204(2018), 110–127.
- Wang, J., Dong, J., Wang, S., Zhang, L., He, H., Yi, Y., Lu, G., Oyler, J., Smith, W.K. and Zhao, M. (2017) Decreasing net primary production due to drought and slight decreases in solar radiation in China from 2000 to 2012. *Journal of Geophysical Research: Atmospheres*, 122, 261–278. <https://doi.org/10.1002/2016JG003417>.
- Wang, S., Xing, J., Zhao, B., Jang, C. and Hao, J. (2014) Effectiveness of national air pollution control policies on the air quality in metropolitan areas of China. *Journal of Environmental Sciences*, 26(1), 13–22. [https://doi.org/10.1016/S1001-0742\(13\)60381-2](https://doi.org/10.1016/S1001-0742(13)60381-2).
- Wielicki, B.A., Barkstrom, B.R., Harrison, E.F., Lee, R.B., III, Smith, G. L. and Cooper, J.E. (1996) Clouds and the Earth's radiant energy system (CERES): an earth observing system experiment. *Bulletin of the American Meteorological Society*, 77, 853–868. [https://doi.org/10.1175/1520-0477\(1996\)077<0853:CATERE>2.0.CO;2](https://doi.org/10.1175/1520-0477(1996)077<0853:CATERE>2.0.CO;2).
- Xing, J., Mathur, R., Pleim, J., Hogrefe, C., Gan, C.-M., Wong, D.C., Wei, C. and Wang, J. (2015) Air pollution and climate response to aerosol direct radiative effects: a modeling study of decadal trends across the northern hemisphere. *Journal of Geophysical Research – Atmospheres*, 120, 12221–12236. <https://doi.org/10.1002/2015JD023933>.
- Xing, J., Pleim, J., Mathur, R., Pouliot, G., Hogrefe, C., Gan, C.M. and Wei, C. (2013) Historical gaseous and primary aerosol emissions in the United States from 1990 to 2010. *Atmospheric Chemistry and Physics*, 13, 7531–7549. <https://doi.org/10.5194/acp-13-7531-2013>.
- Yang, Y., Liao, H. and Lou, S. (2016) Increase in winter haze over eastern China in recent decades: roles of variations in meteorological parameters and anthropogenic emissions. *Journal of Geophysical Research – Atmospheres*, 121, 13050–13065. <https://doi.org/10.1002/2016JD025136>.
- Yang, Y., Wang, H., Smith, S.J., Zhang, R., Lou, S., Yu, H., et al. (2018) Source apportionments of aerosols and their direct radiative forcing and long-term trends over continental United States. *Earth's Future*, 6, 793–808. <https://doi.org/10.1029/2018EF000859>.
- Zarzycki, C.M. and Bond, T.C. (2010) How much can the vertical distribution of black carbon affect its global direct radiative forcing? *Geophysical Research Letters*, 37(20), L20807.
- Zhang, J., Christopher, S.A., Remer, L.A. and Kaufman, Y.J. (2005) Shortwave aerosol radiative forcing over cloud-free oceans from Terra: 2. Seasonal and global distributions. *Journal of Geophysical Research*, 110, D10S24. <https://doi.org/10.1029/2004JD005009>.
- Zhao, B., Jiang, J.H., Diner, D., Worden, J., Liou, K.N., Su, H., Xing, J., Garay, M. and Huang, L. (2017) Decadal-scale trends in regional aerosol particle properties and their linkage to emission changes. *Environmental Research Letters*, 12, 054021.

SUPPORTING INFORMATION

Additional supporting information may be found online in the Supporting Information section at the end of this article.

How to cite this article: Subba T, Gogoi MM, Pathak B, Bhuyan PK, Babu SS. Recent trend in the global distribution of aerosol direct radiative forcing from satellite measurements. *Atmos Sci Lett*. 2020;21:e975. <https://doi.org/10.1002/asl.975>